

Simulation of gas phase reactions for microcrystalline silicon films fabricated by PECVD*

HE Bao-hua (何宝华), YANG Shi-e (杨仕娥)**, CHEN Yong-sheng (陈永生), and LU Jing-xiao (卢景霄)

Key Laboratory of Materials Physics, Education Ministry of China, College of Physics and Engineering, Zhengzhou University, Zhengzhou 450052, China

(Received 31 October 2010)

©Tianjin University of Technology and Springer-Verlag Berlin Heidelberg 2011

We present a numerical gas phase reaction model for hydrogenated microcrystalline silicon ($\mu\text{c-Si:H}$) films from SiH_4 and H_2 gas mixtures with plasma enhanced chemical vapor deposition (PECVD). Under the typical $\mu\text{c-Si:H}$ deposition conditions, the concentrations of the species in the plasma are calculated and the effects of silane fraction ($SF=[\text{SiH}_4]/[\text{H}_2+\text{SiH}_4]$) are investigated. The results show that SiH_3 is the key precursor for $\mu\text{c-Si:H}$ films growth, and other neutral radicals, such as Si_2H_5 , Si_2H_4 and SiH_2 , may play some roles in the film deposition. With the silane fraction increasing, the precursor concentration increases, but H atom concentration decreases rapidly, which results in the lower H/ SiH_3 ratio.

Document code: A **Article ID:** 1673-1905(2011)03-0198-4

DOI 10.1007/s11801-011-0127-7

Hydrogenated microcrystalline silicon ($\mu\text{c-Si:H}$) thin films are promising materials for a wide range of applications in solar cells and thin film transistors. The plasma enhanced chemical vapor deposition (PECVD) from SiH_4 diluted with H_2 is commonly used to deposit $\mu\text{c-Si:H}$ thin films. Although the growth rate has been increased greatly and the film quality has been improved in recent years, the fundamental mechanism of $\mu\text{c-Si:H}$ film growth with PECVD is still poorly understood^[1]. Kessel et al^[2] have suggested that SiH_3 is the dominant radical for $\mu\text{c-Si:H}$ film growth because the SiH_3 concentration is at least an order of magnitude higher than the Si and SiH concentrations for all H_2 dilution ratios. Amanatides et al^[3] have reported that in the case of high H_2 dilution, the highly sticking SiH_2 radical is the main precursor; however, in the case of low H_2 dilution, Si_2H_4 radicals play a major role in film growth. Lately, Lee et al^[4] have deposited $\mu\text{c-Si:H}$ films in the presence of an electric field with PECVD and have suggested that SiH_3^+ ions may act as a main precursor responsible for the formation of $\mu\text{c-Si:H}$ films. Recently, several models for hydrogenated amorphous silicon (a-Si:H) film deposition have been developed and the simulation results are in good agreement with experiments^[5,6]. A few models for $\mu\text{c-Si:H}$ film growth have been reported^[7,8], but they are

not comparable because of different study purposes.

In this paper, we present a well-mixed reaction model to investigate the PECVD process of $\mu\text{c-Si:H}$ film from SiH_4 and H_2 gas mixtures. In order to simplify the calculation, the gas phase transport process is neglected, and it is assumed that all chemical species, electrons and ions are perfectly mixed and uniform throughout the reactor volume, and the electron temperature T_e follows Boltzmann distribution. The model includes 15 radicals, neutral particles and ions, and 50 electron-neutral, neutral-neutral and ion-ion reactions, as shown in Tab.1.

The rate constant for these reactions can be calculated from Arrhenius expression^[8],

$$k=AT^n \exp(-E/R_g T), \quad (1)$$

where the pre-exponential factor A is in unit of $\text{m}^3\text{mol}^{-1}\text{s}^{-1}$, T is the gas temperature (K) or the average electron temperature (eV), n is the temperature exponent, E is the reaction activation energy (J/mol) and $R_g = 8.314 \text{ J}/(\text{mol}\cdot\text{K})$ is the ideal gas constant. The parameters shown in Tab.1 are taken from Refs. [8-11] (The values of n are not given in Tab.1.).

* This work has been supported by the State Key Development Program for Basic Research of China (No.2006CB202601), the National Natural Science Foundation of China (No.51007082), and the Natural Science Foundation of Henan Province (No.072300410080).

** E-mail: yangshie@zzu.edu.cn

Tab.1 Gas phase reactions used in this model

Reaction	$A(\text{m}^3\text{mol}^{-1}\text{s}^{-1})$	$E(\text{J/mol})$
1 $e+\text{H}_2 \rightarrow 2\text{H}+e$	3.43×10^9	7.06×10^5
2 $e+\text{SiH}_4 \rightarrow \text{SiH}_3+\text{H}+e$	9.00×10^9	9.64×10^5
3 $e+\text{SiH}_4 \rightarrow \text{SiH}_2+2\text{H}+e$	1.08×10^9	9.64×10^5
4 $e+\text{SiH}_4 \rightarrow \text{SiH}+\text{H}_2+\text{H}+e$	2.00×10^8	1.03×10^6
5 $e+\text{SiH}_4 \rightarrow \text{SiH}_3^++\text{H}+2e$	1.98×10^9	1.16×10^6
6 $e+\text{SiH}_4 \rightarrow \text{SiH}_2^++\text{H}_2+2e$	2.82×10^9	1.16×10^6
7 $e+\text{SiH}_4 \rightarrow \text{SiH}_3^++\text{H}$	9.09×10^6	8.68×10^5
8 $e+\text{SiH}_4 \rightarrow \text{SiH}_2^++\text{H}_2$	5.40×10^6	8.68×10^5
9 $e+\text{H}_2 \rightarrow \text{H}_2^++2e$	1.00×10^9	1.00×10^6
10 $\text{H}+\text{SiH}_4 \rightarrow \text{SiH}_3+\text{H}_2$	1.07×10^8	1.60×10^4
11 $\text{H}+\text{Si}_2\text{H}_6 \rightarrow \text{Si}_2\text{H}_5+\text{H}_2$	2.26×10^7	1.60×10^4
12 $\text{H}+\text{Si}_3\text{H}_8 \rightarrow \text{SiH}_3+\text{Si}_2\text{H}_6$	6.87×10^7	1.60×10^4
13 $\text{H}+\text{Si}_4\text{H}_{10} \rightarrow \text{SiH}_4+\text{SiH}_3$	4.52×10^7	1.60×10^4
14 $\text{SiH}_3+\text{Si}_2\text{H}_6 \rightarrow \text{SiH}_4+\text{Si}_2\text{H}_5$	2.40×10^8	2.08×10^4
15 $\text{SiH}_3+\text{SiH}_3 \rightarrow \text{SiH}_4+\text{SiH}_2$	1.00×10^8	0
16 $\text{SiH}_3+\text{SiH}_3 \rightarrow \text{H}_2+\text{Si}_2\text{H}_4$	3.49×10^6	0
17 $\text{SiH}_3+\text{Si}_2\text{H}_5 \rightarrow \text{Si}_3\text{H}_8$	3.31×10^7	0
18 $\text{SiH}_3+\text{SiH}_4 \rightarrow \text{Si}_2\text{H}_5+\text{H}_2$	1.75×10^6	1.84×10^4
19 $\text{SiH}_3+\text{Si}_3\text{H}_8 \rightarrow \text{Si}_3\text{H}_9+\text{SiH}_4$	1.50×10^6	0
20 $\text{SiH}_3+\text{Si}_4\text{H}_{10} \rightarrow \text{Si}_4\text{H}_{11}+\text{H}_2$	1.20×10^6	0
21 $\text{SiH}_3+\text{Si}_4\text{H}_{10} \rightarrow \text{SiH}_4+\text{Si}_4\text{H}_9$	4.52×10^6	0
22 $\text{SiH}_3+\text{Si}_3\text{H}_7 \rightarrow \text{Si}_4\text{H}_{10}$	1.20×10^6	0
23 $\text{SiH}_2+\text{H}_2 \rightarrow \text{SiH}_4$	5.48×10^7	8.37×10^3
24 $\text{SiH}_2+\text{SiH}_4 \rightarrow \text{Si}_2\text{H}_6$	6.03×10^8	5.40×10^3
25 $\text{SiH}_2+\text{Si}_2\text{H}_6 \rightarrow \text{Si}_3\text{H}_8$	3.97×10^9	8.37×10^3
26 $\text{SiH}_2+\text{Si}_3\text{H}_8 \rightarrow \text{Si}_4\text{H}_{10}$	1.30×10^8	0
27 $\text{SiH}_2+\text{Si}_4\text{H}_{10} \rightarrow \text{Si}_5\text{H}_{12}$	1.30×10^8	0
28 $\text{SiH}+\text{SiH}_4 \rightarrow \text{Si}_2\text{H}_5$	4.27×10^7	8.37×10^3
29 $\text{SiH}+\text{H}_2 \rightarrow \text{SiH}_3$	3.43×10^7	8.37×10^3
30 $\text{SiH}+\text{Si}_2\text{H}_6 \rightarrow \text{Si}_3\text{H}_8$	4.52×10^8	8.37×10^3
31 $\text{SiH}_4+\text{Si}_2\text{H}_4 \rightarrow \text{Si}_3\text{H}_8$	9.63×10^5	8.37×10^3
32 $\text{SiH}_4+\text{Si}_2\text{H}_5 \rightarrow \text{SiH}_3+\text{Si}_2\text{H}_6$	9.03×10^4	8.37×10^3
33 $\text{SiH}_4+\text{Si}_3\text{H}_7 \rightarrow \text{Si}_3\text{H}_8+\text{SiH}_3$	8.43×10^3	0
34 $\text{SiH}_4+\text{Si}_4\text{H}_9 \rightarrow \text{SiH}_3+\text{Si}_4\text{H}_{10}$	5.66×10^3	0
35 $\text{H}_2+\text{Si}_2\text{H}_4 \rightarrow \text{SiH}_4+\text{SiH}_2$	1.87×10^6	8.37×10^3
36 $\text{H}_2+\text{Si}_2\text{H}_4 \rightarrow \text{Si}_2\text{H}_6$	2.41×10^6	8.37×10^3
37 $\text{Si}_2\text{H}_5+\text{Si}_2\text{H}_5 \rightarrow \text{Si}_2\text{H}_6+\text{Si}_2\text{H}_4$	2.59×10^8	8.37×10^3
38 $\text{Si}_2\text{H}_5+\text{Si}_4\text{H}_9 \rightarrow \text{Si}_6\text{H}_{14}$	7.23×10^6	8.37×10^3
39 $\text{Si}_2\text{H}_5+\text{Si}_2\text{H}_4 \rightarrow \text{Si}_4\text{H}_9$	1.20×10^6	0
40 $\text{Si}_2\text{H}_5+\text{Si}_3\text{H}_7 \rightarrow \text{Si}_5\text{H}_{12}$	1.20×10^7	0
$\text{Si}_2\text{H}_4+\text{Si}_n\text{H}_{2n+2} \rightarrow \text{Si}_{n+2}\text{H}_{2n+6}$	6.62×10^4	0
$e+\text{SiH}_n^+ \rightarrow \text{SiH}_{n-1}+\text{H}$	1.5×10^{11}	0
$\text{SiH}_m^++\text{SiH}_n \rightarrow \text{SiH}_m+\text{SiH}_n$	3.0×10^{11}	0
$\text{SiH}_m^++\text{H}_2 \rightarrow \text{SiH}_m+\text{H}_2$	3.0×10^{11}	0
$\text{H}_2^++\text{SiH}_4 \rightarrow \text{SiH}_3^++\text{H}_2$	1.8×10^9	0

The gas phase reaction rate R can be obtained by

$$R=kC_1C_2, \quad (2)$$

where C_1 and C_2 represent the concentrations of reactants in unit of mol/m^3 .

In this model, the input parameters, such as the gas

temperature, gas pressure, average electron temperature, electron density, and hydrogen concentration, are kept unchanged at 500 K, 600 Pa, 2 eV, $8.3 \times 10^{-8} \text{ mol/m}^3$, and $1.69 \times 10^{-2} \text{ mol/m}^3$, respectively. Firstly, we investigate the concentrations of the chemical species in the plasma when the silane fraction ($SF = [\text{SiH}_4]/[\text{H}_2+\text{SiH}_4]$) is fixed at 3%, as shown in Fig. 1, where solid and broken lines denote neutral particles and ions, respectively. It should be pointed out that only species, which are with high concentrations or dominant in film growth, are plotted.

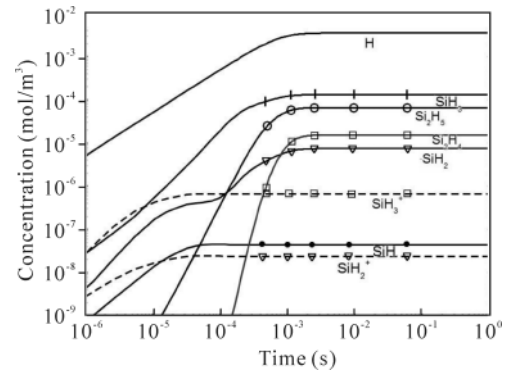


Fig.1 Species concentrations in the plasma versus time

According to the model, all species concentrations increase with time, and then tend to be saturated after 10^{-3} s, which means that the stable plasma is formed. The hydrogen atom concentration is the maximum, equal to $3.5 \times 10^{-3} \text{ mol/m}^3$, at the silane fraction of 3%. It can be seen in Tab.1 that two hydrogen atoms are generated during each H_2 dissociation reaction in Reaction 1. In addition, all the dissociation reactions of silane molecules in Reactions 2-4 can release hydrogen atoms. At the same time, under the condition of low silane fraction, the rate of hydrogen atom abstraction reaction in Reaction 10 is low, which results in annihilation of hydrogen atoms. Among the neutral radicals, the SiH_3 concentration is the maximum, then that of Si_2H_5 , Si_2H_4 and SiH_2 in order. Because both the electron dissociation of silane and the hydrogen abstraction create SiH_3 radicals. On the other hand, the rate constants of secondary gas phase reactions for SiH_3 are lower compared with SiH_2 and SiH . The concentrations of SiH_3^+ and SiH_2^+ are very low, which is attributed to their high reaction activation energy values.

The silane fraction has important effects on the deposition rate, crystalline fraction and electrical properties of $\mu\text{-Si:H}$ films. With other parameters fixed, increasing silane fraction can induce the phase transition from $\mu\text{-Si:H}$ to a-Si:H films^[12]. Commonly, it is assumed that the neutral radical SiH_3 is most abundant species in the plasma and acts as the main precursor for a-Si:H film growth^[13]. In order to determine the $\mu\text{-Si:H}$ film deposition precursors, we investigate

the dependence of the species concentrations on the silane fraction ranging from 1% to 10%. The results are shown in Fig.2. When the silane fraction increases, the concentrations of silicon hydrides, such as SiH₃, Si₂H₅, Si₂H₄ and SiH₂, all increase in different magnitudes, while hydrogen atom concentration decreases rapidly. It should be noted that the order of the species concentrations in Fig.2 does not change with the silane fraction increasing. Among the silane radicals, the SiH₃ concentration is the maximum at each silane fraction, which is 1–2 orders of magnitude higher than that of SiH₂.

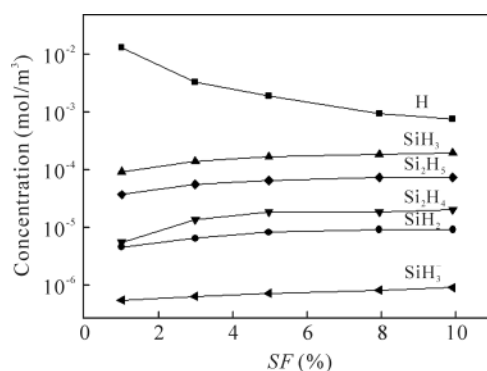


Fig.2 Species concentrations versus silane fraction

With fixed n_e value, the rates of reactions such as 2, 3, 16 and 18 in Tab.1 increase with silane fraction increasing. As for the products of these reactions, the silicon hydrides concentrations increase too. Under the higher silane fraction, the abstraction reaction ($H + SiH_4 \rightarrow SiH_3 + H_2$) not only produces more SiH₃ radicals, but also consumes a lot of hydrogen atoms, which results in the decline of hydrogen atom concentration in Fig.2.

It should be pointed out that each radical in the plasma has different surface reaction probabilities β [2,14]. For example, SiH has the maximum reaction probability, $\beta_{SiH} \approx 0.95$, followed by SiH₂ and Si₂H₄, about 0.6, while that of SiH₃ is lower, generally $\beta_{SiH_3} \approx 0.2$ used. From the results shown in Fig.2 and the above-mentioned surface reaction probabilities, we suggest that SiH₃ is the key precursor for μc -Si:H film growth, similar to a-Si:H, and other neutral radicals such as Si₂H₅, Si₂H₄ and SiH₂ may play some roles in the film deposition. In addition, the concentration of SiH₃⁺ ion remains rather lower at each silane fraction, so it has little contribution to the film growth. The results are consistent with the conclusions of Kessel et al from their experiments[2].

Experimental results have been reported that with the increase of silane fraction, the deposition rate of the μc -Si:H film increases, while crystallinity becomes worse[12]. Obviously, the increase in deposition rate is due to the increase in the concentration of dominant precursors for growth (typically SiH₃). The decrease in the crystalline fraction is

due to the decrease in hydrogen atom concentration, which results in the lower H/SiH₃ ratio, as shown in Fig.3. The optical emission spectroscopy (OES) is commonly used to monitor the emission intensities of H α , H β , Si* and SiH* in the plasma, in which Si* or SiH* emission intensity is proportional to the precursor concentration[15]. Rath et al[16] reported that the crystalline fraction decreases with the decline of H α /Si* ratio, and the film changes from microcrystalline to amorphous phase when H α /Si* ratio exceeds a critical value. It is well known that hydrogen atoms play a crucial role in the growth of the silicon films. With the decrease of hydrogen atom concentration in the plasma, the coverage rate of hydrogen atoms at the growing surface is reduced, which results in the decrease of surface diffusion coefficients of the deposition precursors. On the other hand, the role of hydrogen atoms etching the weak Si-Si bonds in the a-Si:H network declines, which results in the crystallinity deterioration.

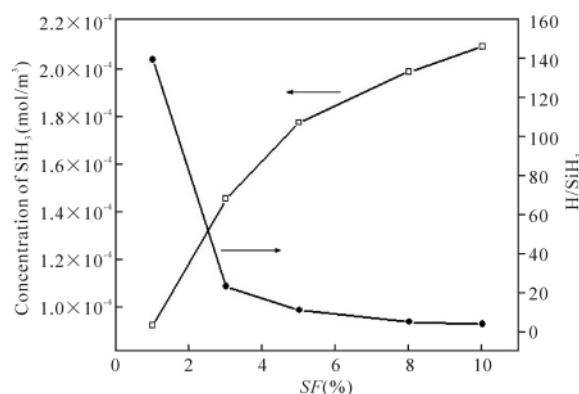


Fig.3 SiH₃ concentration and H/SiH₃ ratio versus silane fraction

In summary, a numerical gas phase reaction model for μc -Si:H film growth from SiH₄ and H₂ gas mixtures with PECVD is presented. The simulation results indicate that hydrogen and SiH₃ are the dominant species in the plasma for μc -Si:H film deposition. Similar to the case of a-Si:H, SiH₃ is the key precursor for μc -Si:H film growth. With the increase of silane fraction, the precursor concentrations increase, which is the main reason for the enhancement of the growth rate; at the same time, the hydrogen atom concentration decreases rapidly and H/SiH₃ ratio declines, which is the reason for the decrease of the film crystalline fraction.

References

[1] Matsuda A, Thin Solid Films **337**, 1 (1999).
 [2] Kessels W M M, Nadir K and van de Sanden M C M, J. Appl. Phys. **99**, 110 (2006).
 [3] Amanatides E, Stamou S and Mataras D, J. Appl. Phys. **90**, 5786 (2001).
 [4] Joon-Yong Lee and Jong-Hwan Yoon, Solid State Communi-

- cations **132**, 627 (2004).
- [5] Nienhuisa G J, Goedheer W J and Hamers E A G, *J. Appl. Phys.* **82**, 2060 (1997).
- [6] Kathleen De Bleecker, Annemie Bogaerts, Wim Goedheer and Renaat Gijbelsa, *IEEE Transactions on Plasma Science* **32**, 691 (2004).
- [7] Zhang Fa-rong, Zhang Xiao-dan, Amanatides E, Matras D and Zhao Ying, *Journal of Optoelectronics • Laser* **19**, 208 (2008). (in Chinese)
- [8] Koji Satakea and Yasuyuki Kobayashi, *J. Appl. Phys.* **97**, 23308 (2005).
- [9] Moravej M, Babayan S E, Nowling G R, Yang X and Hicks R F, *Plasma Sources Science and Technology* **13**, 8 (2004).
- [10] Kushner M J, *J. Appl. Phys.* **63**, 25 (1988).
- [11] Allen W N, Cheng T M H and Lampe F W, *J. Chem. Phys.* **66**, 3371 (1997).
- [12] Mai Yaohua, *Microcrystalline Silicon Layers for Thin Film Solar Cells Prepared with PECVD and HWCVD*, Tianjin: Photonics Research Institute, Nankai University, 46 (2006). (in Chinese)
- [13] Sriraman S, Agarwal S, Aydil E S and Maroudas D, *Nature* **418**, 6265 (2002).
- [14] Kessels W M M, van de Sanden M C M, Severens R J and Schram D C, *J. Appl. Phys.* **87**, 3313 (2000).
- [15] Zhu Feng, Zhang Xiaodan, Zhao Ying, Wei Changchun, Sun Jian and Geng Xinhua, *Chinese Journal of Semiconductors* **25**, 1624 (2004). (in Chinese)
- [16] Rath J K, Franken R H J, Gordijn A, Schropp R E I and Goedheer W J, *Journal of Non-Crystalline Solids* **60**, 338 (2004).